

Depolarization field mitigated domain engineering in nickel diffused lithium tantalate

L.-H. Peng, Y.-P. Tseng, K.-L. Lin, Z.-X. Huang, C.-T. Huang, and A.-H. Kung

Citation: *Applied Physics Letters* **92**, 092903 (2008); doi: 10.1063/1.2890728

View online: <http://dx.doi.org/10.1063/1.2890728>

View Table of Contents: <http://scitation.aip.org/content/aip/journal/apl/92/9?ver=pdfcov>

Published by the [AIP Publishing](#)

Articles you may be interested in

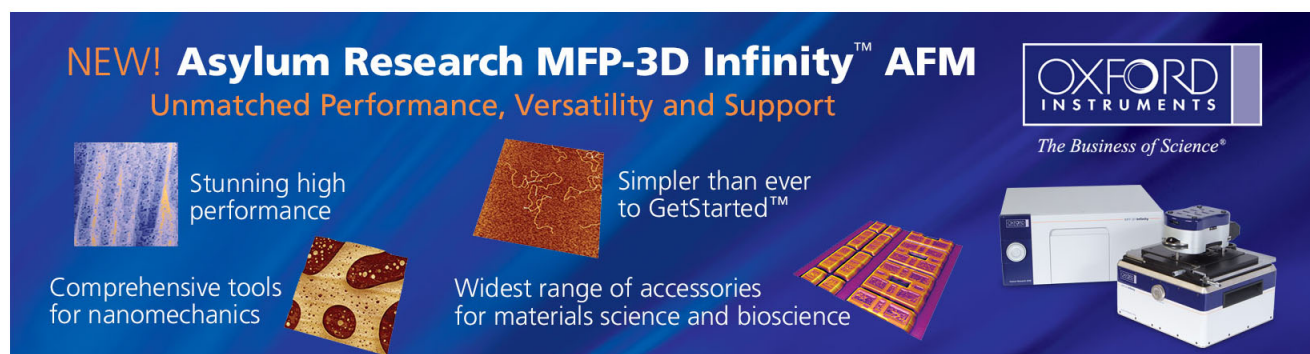
[Electron-beam-induced domain poling in Li Nb O 3 for two-dimensional nonlinear frequency conversion](#)
Appl. Phys. Lett. **88**, 011103 (2006); 10.1063/1.2159089

[Mitigation of transverse domain growth in two-dimensional polarization switching of lithium niobate](#)
Appl. Phys. Lett. **81**, 5210 (2002); 10.1063/1.1533115

[Surface domain engineering in congruent lithium niobate single crystals: A route to submicron periodic poling](#)
Appl. Phys. Lett. **81**, 4946 (2002); 10.1063/1.1532773

[Backswitch poling in lithium niobate for high-fidelity domain patterning and efficient blue light generation](#)
Appl. Phys. Lett. **75**, 1673 (1999); 10.1063/1.124787

[Application of the second harmonic generation microscope to nondestructive observation of periodically poled ferroelectric domains in quasi-phase-matched wavelength converters](#)
J. Appl. Phys. **81**, 369 (1997); 10.1063/1.364121

The advertisement features a dark blue background with white and orange text. At the top left, it reads 'NEW! Asylum Research MFP-3D Infinity™ AFM' in large white letters, followed by 'Unmatched Performance, Versatility and Support' in orange. To the right is the Oxford Instruments logo, which includes the text 'OXFORD INSTRUMENTS' and the tagline 'The Business of Science®'. Below the main text are four images: a blue textured surface, a brown textured surface, a grid of colorful squares, and a photograph of the AFM instrument. Each image is accompanied by a short text description: 'Stunning high performance', 'Simpler than ever to GetStarted™', 'Comprehensive tools for nanomechanics', and 'Widest range of accessories for materials science and bioscience'.

Depolarization field mitigated domain engineering in nickel diffused lithium tantalate

L.-H. Peng,^{1,a)} Y.-P. Tseng,¹ K.-L. Lin,¹ Z.-X. Huang,¹ C.-T. Huang,¹ and A.-H. Kung^{2,3}

¹Department of Electrical Engineering and Institute of Photonics and Optoelectronics, National Taiwan University, Taipei 106, Taiwan, Republic of China

²Institute of Atomic and Molecular Sciences, Academia Sinica, Taipei 106, Taiwan, Republic of China

³Department of Photonics, ChiaoTung University, Hsinchu 300, Taiwan, Republic of China

(Received 7 January 2008; accepted 5 February 2008; published online 4 March 2008)

We demonstrated a domain reversal mechanism on Z-cut congruent-grown lithium tantalate (LiTaO₃) composed of nickel (Ni) diffusion followed by pulse field poling. Domain nucleation and forward growth were found confined to the nondiffused regions, where the commonly observed serrated domain fronts in poled LiTaO₃ were absent in this work. These observations are ascribed to the formation of domain nucleation barrier by the depolarization field and reveal the divergence effect in the ferroelectric spontaneous polarization at the domain boundary due to Ni diffusion. This mechanism simplifies the fabrication of periodically poled LiTaO₃ for second-harmonic generation in the blue spectral regime. © 2008 American Institute of Physics. [DOI: 10.1063/1.2890728]

Ferroelectric crystals are characterized by the reversibility of spontaneous polarization (\mathbf{P}_s) when subject to an external electric field poling above the crystal's coercive field E_c .¹ The capability for ferroelectrics to retain a periodically poled domain structure with alternating sign change in \mathbf{P}_s can substantially modify the material's tensor properties.² This effect can lead to a realization of high-density nonvolatile memory devices due to fast polarization switching in ferroelectric thinfilms.³ Periodic sign reversal in \mathbf{P}_s can further impose on the ferroelectric a structure-related vector to compensate the phase mismatch in a nonlinear wave mixing process. This mechanism is known as quasi-phase-matching⁴ (QPM) and has been recently applied to second-harmonic generation⁵ (SHG) and third-harmonic generation⁶ and optical parametric oscillation (OPO).⁷ Compared with the conventional birefringent phase matching scheme, the QPM method offers a higher conversion efficiency due to access to the largest nonlinear susceptibility tensor $\chi_{33}^{(2)}$ and absence of beam walk off.⁸ Recent studies further clarify the advantages of using two-dimensionally (2D) poled ferroelectric nonlinear photonic crystals⁹ to achieve broad acceptance bandwidth in the spectral-tuning¹⁰ and temperature-tuning¹¹ range, and interesting optical phenomena such as cascade,¹² conic,¹³ and Čerenkov¹⁴ generation in the QPM process.

These observations prompt a need of domain engineering to deploy a desirable pattern transfer in the electrically poled ferroelectrics. A typical structure composed of an insulator pattern over gratinglike metallic contact or vice versa has been demonstrated for the poling electrode.⁷ The polarization switching process is known to initiate underneath the corrugated edge of the electrode thus made. The corresponding domain nucleation rate has been found proportional to $\sim \exp(-\alpha/E_z)$, where α represents a phenomenological activation term and E_z the poling field.¹⁵ The kinetics of domain reversal is known to consist of a fast domain forward growth followed by a sidewise motion.¹⁶ Conventional wisdom further suggests a use of pulse field shaping such as back

switching¹⁷ to mitigate the polarization switching process.

Caution, however, arises from frequent observation of unbounded expansion and merging of inverted domains in periodically poled lithium niobate (LiNbO₃) and lithium tantalate (LiTaO₃).¹⁸ For example, merging of inverted domains in LiTaO₃ can result in a serrated front which displays an order of magnitude increase in the wall velocity.¹⁹ This hampers the development of fine-pitch poled LiTaO₃ as the device lateral homogeneity decreases along the crystal's polar axis.²⁰ Examination of the electrostatic field distribution indicates that the driving force of domain broadening is due to the fringing field effect.²¹ The latter reflects field distortion due to bending of the equal potential line across the corrugated ferroelectric/electrode interface.²² Such distorted field line can extend beyond the electrode contact window and cause domain broadening.²³

In this work, we demonstrate a ferroelectric poling scheme on congruent-grown LiTaO₃ that can be immune to the aforementioned shortcomings. It is based upon Landauer's nucleation theory in which bound charges, arising from the divergence of \mathbf{P}_s at the domain boundary, can constitute a nucleation barrier to prohibit the nucleation of inverted domain and its forward growth.²⁴ With a moderate bound charge density $\sim 1 \mu\text{C}/\text{cm}^2$, a large depolarization field $\sim 10^7 \text{ V}/\text{cm}$ has been estimated at the domain boundary.²⁵ This number is two orders of magnitude higher than the crystal's coercive field and can, thus, inhibit the applied field from initiating domain reversal. It has further been noted that between pairs of charged boundaries, the field line due to electrostatic repulsion can facilitate the confinement of lateral domain motion.²⁶

A crucial part of device processing as proposed in this work is to prepare a periodic distribution of positively bound charges underneath the +Z surface of LiTaO₃. A "head-to-head" configuration of \mathbf{P}_s can act as a source of bound charge due to the divergence effect of \mathbf{P}_s , viz., $\nabla \cdot \mathbf{P}_s = -\rho$, as inferred from the electrostatics analysis.^{24,26} Such bound charges, when not screened by the injected carriers, can produce a depolarization field to constrain the nucleation and motion of the inverted domain. A head-to-head domain con-

^{a)}Electronic mail: peng@cc.ee.ntu.edu.tw.

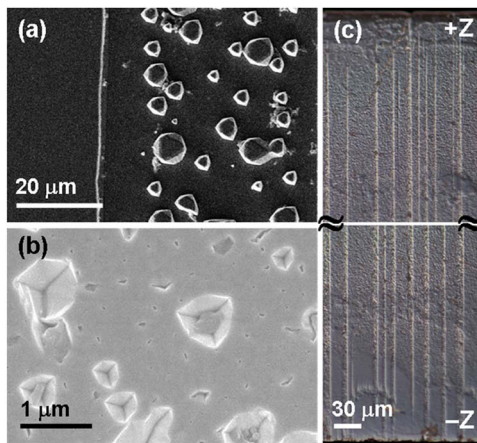


FIG. 1. (Color online) SEM micrographs of the etched (a) $-Z$ and (b) $+Z$ faces of poled LiTaO_3 sample A with right half of its $+Z$ face diffused with Ni prior to proceed with electric poling. (c): Cross-sectional optical micrograph taken from the right half side of sample A showing a straight growth of inverted domains through the 0.5 mm thick substrate.

figuration can be realized by introducing a shallow inverted domain in the virgin ferroelectric crystal. This type of domain configuration has been reported on the $+Z$ face of LiNbO_3 by using titanium (Ti) in diffusion²⁵ or lithium (Li) out diffusion²⁷ at a temperature higher than 1050 °C. However, similar heat treatment on LiTaO_3 at ~ 600 °C, which is below the crystal's Curie temperature, failed to create such inverted domains.²⁸ The reason has been attributed to the lack of activated diffusion process with which the impurity-gradient induced field is insufficient to initiate the polarization switching.

To resolve this issue, we seek solutions from a nickel (Ni) diffusion process which has been applied to make waveguides in LiTaO_3 .²⁹ Testing electrodes made of ~ 15 nm thick Ni layer or grating were prepared on the $+Z$ face of 0.5 mm thick congruent-grown LiTaO_3 substrates.³⁰ The samples were then placed inside a box furnace and subject to heat treatment at 570 °C for ~ 5 h in air ambient. High-voltage pulses of ~ 13 kV were then delivered to the sample surface through contact with de-ionized water. For surface morphology and profilometry analysis of the domain structure, the polished samples were etched in hydrofluoride (HF) for ~ 3 h and examined by scanning electron microscope (SEM) and atomic force microscope (AFM).

First shown in Fig. 1(a) is the SEM micrograph taken from the etched $-Z$ face of a poled LiTaO_3 Sample A whose *right* half plane in the crystal's $+Z$ face was diffused with Ni prior to proceed with electric poling. Referring to Fig. 1(a), a sparse distribution of triangular shape of hillocks corresponding to the inverted domains are discernible in the right half plane of the sample's $-Z$ face; whereas uniformly poled domains are observed in the other left half plane. Further evidence revealing the Ni-affiliated domain poling process can be found from the magnified SEM micrograph of etch pits shown in Fig. 1(b). In the latter case, the micrograph was taken from the right half plane of Sample A's $+Z$ face. The etch pits shown here exhibit a size distribution in the nanometer to submicron regime and an invert-pyramid shape complementary to that observed in Fig. 1(a). They represent nuclei of inverted domains which respond to electric poling in the Ni-diffused region over the $+Z$ face LiTaO_3 . It further suggests that the fissurelike structure in an oxidized metallic

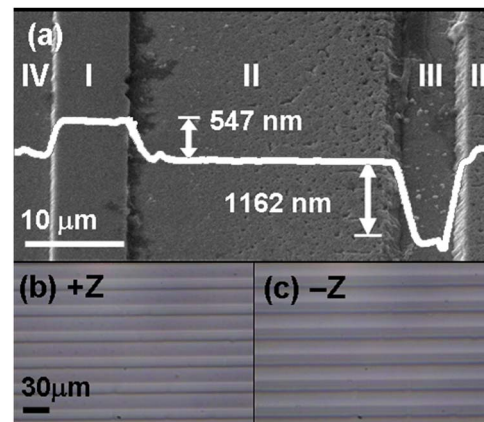


FIG. 2. (Color online) (a) AFM surface profilometry taken from the $+Z$ face of periodically poled LiTaO_3 sample B and overlaid with the SEM micrograph. Region I: nondiffused, nonpoled. Region II: Ni-diffused, electrically poled. Region III: nondiffused, electrically poled. Region IV: Ni-diffused, nonpoled. (b) $+Z$ and (c) $-Z$ face micrograph of an electrically poled LiTaO_3 sample with Ni-diffused electrode of 29 μm period.

film can act an electric path to the underlying ferroelectric surface and serve as nucleation site to initiate domain reversal.²⁶ This mechanism is confirmed in Fig. 1(c) where the cross-sectional optical micrograph taken from the right half side of sample A exhibits a straight forward growth of inverted domains through the 0.5 mm thick substrate. One can therefore conclude from Fig. 1 that for regions diffused with Ni there appears a barrier to inhibit the occurrence of polarization switching.

A possible link between the Ni diffusion and the polarization switching of LiTaO_3 is via the depolarization field to inhibit the nucleation of inverted domain. This proposed mechanism can be verified by examining the etch profile of periodically poled LiTaO_3 samples diffused with Ni electrodes. As example, in Fig. 2, we overlay the (a) AFM surface profilometry data with (b) SEM micrograph taken upon the etched $+Z$ face of a periodically poled LiTaO_3 sample B diffused with a ~ 29.5 μm period of Ni grating. We first note a presence of the virgin LiTaO_3 crystal's polarization state ($+P_s$) in the nondiffused and unpoled region I. The latter serves as a level reference as an etch depth of ~ 0.55 μm can be inferred from all of the Ni-diffused regions II regardless it has been electrically poled or not. This observation suggests that the Ni-diffusion region is characterized with negative polarization state. In comparison, a ~ 1.7 μm etch depth associated with electrically poled domains is observed in the non-Ni diffused region III. It reveals a spatial confinement of the electrically poled domains (region III) bounded by the Ni-diffusion layer (region II), suggesting that the latter acts as a barrier to prohibit lateral domain motion. This analysis is further confirmed in Figs. 2(b) and 2(c) where the $+Z$ and $-Z$ face optical micrographs of another set of periodically poled LiTaO_3 Sample using Ni-diffused grating electrodes exhibit a $\sim 50\%$ duty cycle in the poled domain structure. Furthermore, by closely examining the surface morphology of Fig. 2(a), one can identify the etch stop surface in the Ni-diffused layer (region II) to be associated with the positive domain side in the $+Z$ face of LiTaO_3 . We also found Ni diffusion in the $-Z$ face of LiTaO_3 (data not shown here) can still retain the etching characteristics of negative polarization state. These analyses verify that the Ni diffusion process in LiTaO_3 , like the case of Ti diffusion in LiNbO_3 ,²⁵ can result

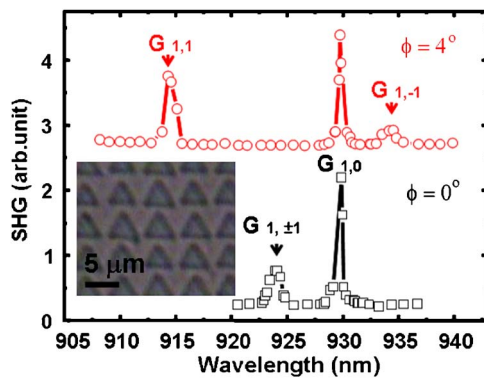


FIG. 3. (Color online) Spectral tuning curve of 2D periodically poled LiTaO₃ sample C with reciprocal vectors $\mathbf{G}_{1,0}$ and $\mathbf{G}_{1,\pm 1}$ participating in the QPM-SHG $2\mathbf{k}_\omega + \mathbf{G}_{\text{mn}} = \mathbf{k}_{2\omega}$ process. Inset: $-Z$ face micrograph of sample C with Ni-diffused electrode at a periodicity of $5.1 \times 5.1 \mu\text{m}^2$.

in shallow surface domain inversion in the $+Z$ face and retain the virgin ferroelectric crystal's polarity in the $-Z$ face. It further supports our proposal by invoking the depolarization field to mediate the polarization switching process and to manipulate the nucleation and motion of inverted domains. In comparison, we note that the commonly used proton exchange method can only result in surface domain inversion on the $-Z$ face of LiTaO₃.³¹ It, however, can severely modify the ferroelectric LiTaO₃ or LiNbO₃ $+Z$ face into a cubic perovskite structure by losing the crystal's spontaneous polarization.^{32,33}

As a further proof of this proposed mechanism in shaping the ferroelectric domain structures, we prepared another set of 2D periodically poled LiTaO₃ sample C with a periodicity of $5.1 \times 5.1 \mu\text{m}^2$. Here, the optical micrograph in the inset of Fig. 3 depicts the periodic domain structure of sample C in the $-Z$ face where 2D array of equilateral triangular domains are clearly observed to reside on the tetragonal lattice sites that have been electrically poled through the 0.5 mm thick substrate. These data provide evidence that the serrated wall front, constantly observed in poled LiTaO₃ due to fast step growth at the merged domain boundaries,^{19,34} is absent in our poling scheme. Last but not the least, we illustrate in Fig. 3 the QPM-SHG wavelength tuning spectra of sample C which matches the generation of 465 nm blue laser. The experiments were conducted by using a home-built green laser pumped OPO with a temperature-tuned periodically poled stoichiometric LiTaO₃ to operate in the 930 nm band. At normal incidence ($\phi=0$) the QPM-SHG process can be fulfilled at a wavelength of 929.5 and 923.5 nm, respectively, by matching the condition of $2\mathbf{k}_\omega + \mathbf{G}_{\text{mn}} = \mathbf{k}_{2\omega}$ at a reciprocal vector of $\mathbf{G}_{1,0}$ and $\mathbf{G}_{1,\pm 1}$. The smaller Fourier component of $\chi^{(2)}(\mathbf{G}_{1,\pm 1})$ accounts for a lower SHG conversion efficiency compared with its counterpart of $\chi^{(2)}(\mathbf{G}_{1,0})$. By slightly rotating the sample at 4° , the degeneracy of QPM-SHG wavelength at $\mathbf{G}_{1,1}$ and $\mathbf{G}_{1,-1}$ splits to 915 and 935 nm. Detailed optical analysis of these 2D poled LiTaO₃ nonlinear photonics crystals will be presented in a forthcoming publication.

In summary, we have demonstrated a method of creating surface inverted domain on the $+Z$ face of LiTaO₃ by Ni

diffusion. By invoking the divergence effect of spontaneous polarization and judiciously manipulating the depolarization field, not only can one suppress the domain nucleation probability but also confine the motion of electrically poled domains to the boundary formed by the Ni diffusion process. This mechanism allows us to fabricate periodically poled LiTaO₃ structures for visible SHG laser applications.

The authors wish to acknowledge supporting from the National Science Council, Grant No. NSC 96-2221-E-002-098.

¹I. Camlibel, *J. Appl. Phys.* **40**, 1690 (1969).

²For a recent review, see, *Micro/nano Engineering and Characterization of Ferroelectric Crystals For Applications in Photonics*, edited by P. Ferraro, S. Grilli, and P. De Natale (Springer, New York, 2008).

³M. Dawber, K. M. Rabe, and J. F. Scott, *Rev. Mod. Phys.* **77**, 1083 (2005).

⁴J. A. Armstrong, N. Bloembergen, J. Ducuing, and P. S. Pershan, *Phys. Rev.* **127**, 1918 (1963).

⁵M. Yamada, N. Nada, M. Saitoh, and K. Watanabe, *Appl. Phys. Lett.* **62**, 435 (1993).

⁶S.-N. Zhu, Y.-Y. Zhu, and N.-B. Ming, *Science* **278**, 843 (1997).

⁷L. E. Myers, R. C. Eckardt, M. M. Fejer, R. L. Byer, W. R. Bosenberg, and J. W. Pierce, *J. Opt. Soc. Am. B* **12**, 2102 (1995).

⁸M. M. Fejer, G. A. Magel, D. H. Jundt, and R. L. Byer, *IEEE J. Quantum Electron.* **28**, 2631 (1992).

⁹V. Berger, *Phys. Rev. Lett.* **81**, 4136 (1998).

¹⁰Y. Sheng, J. Dou, B. Ma, B. Cheng, and D. Zhang, *Appl. Phys. Lett.* **91**, 011101 (2007).

¹¹L.-H. Peng, C.-C. Hsu, and Y.-C. Shih, *Appl. Phys. Lett.* **83**, 3447 (2003).

¹²N. G. R. Broderick, G. W. Ross, H. L. Offerhaus, D. J. Richardson, and D. C. Hanna, *Phys. Rev. Lett.* **84**, 4345 (2000).

¹³P. Xu, S. H. Ji, S. N. Zhu, X. Q. Yu, J. Sun, H. T. Wang, J. L. He, Y. Y. Zhu, and N. B. Ming, *Phys. Rev. Lett.* **93**, 133904 (2004).

¹⁴Y. Zhang, Z. Qi, W. Wang, and S. N. Zhu, *Appl. Phys. Lett.* **89**, 171113 (2006).

¹⁵W. J. Merz, *Phys. Rev.* **95**, 690 (1954).

¹⁶R. C. Miller and G. Weinreich, *Phys. Rev.* **117**, 1460 (1960).

¹⁷R. G. Batchko, V. Y. Shur, M. M. Fejer, and R. L. Byer, *Appl. Phys. Lett.* **75**, 1673 (1999).

¹⁸V. Y. Shur, E. L. Romyantsev, E. V. Nikolaeva, and E. I. Shishkin, *Appl. Phys. Lett.* **77**, 3636 (2000).

¹⁹V. Gopalan and T. E. Mitchell, *J. Appl. Phys.* **85**, 2304 (1999).

²⁰J.-P. Meyn, C. Laue, R. Knappe, R. Wallenstein, and M. M. Fejer, *Appl. Phys. B: Lasers Opt.* **73**, 111 (2001).

²¹G. Rosenman, Kh. Garb, A. Skliar, M. Oron, D. Eger, and M. Katz, *Appl. Phys. Lett.* **73**, 865 (1998).

²²L.-H. Peng, Y.-J. Shih, and Y.-C. Zhang, *Appl. Phys. Lett.* **81**, 1666 (2002).

²³S. Nagano, M. Konishi, T. Shiomi, and M. Minakata, *Jpn. J. Appl. Phys., Part 1* **42**, 4334 (2003).

²⁴R. Landauer, *J. Appl. Phys.* **28**, 227 (1957).

²⁵S. Miyazawa, *J. Appl. Phys.* **50**, 4599 (1979).

²⁶L.-H. Peng, Y.-C. Shih, S.-M. Tsan, and C. C. Hsu, *Appl. Phys. Lett.* **81**, 5210 (2002).

²⁷N. Ohnishi, *Jpn. J. Appl. Phys.* **16**, 1069 (1977).

²⁸K. Nakamura and H. Shimizu, *Appl. Phys. Lett.* **56**, 1535 (1990).

²⁹W.-L. Chen, D.-J. Chen, and W.-S. Wang, *IEEE Photonics Technol. Lett.* **7**, 203 (1995).

³⁰Purchased from www.dqhuaying.com.

³¹K. Mizuuchi, K. Yamamoto, and H. Sato, *J. Appl. Phys.* **75**, 1311 (1994).

³²K. Mizuuchi and K. Yamamoto, *Appl. Phys. Lett.* **66**, 2943 (1995).

³³S. Grilli, C. Canalias, F. Laurell, P. Ferraro, and P. De Natale, *Appl. Phys. Lett.* **89**, 032902 (2006).

³⁴A. Chernykh, V. Shur, E. Nikolaeva, E. Shishkin, A. Shur, K. Terabe, S. Kurimura, K. Kitamura, and K. Gallo, *Mater. Sci. Eng., B* **120**, 109 (2005).